THE JOURNAL OF PHYSICAL CHEMISTRY B

ARTICLE

pubs.acs.org/JPCB

Influence of Denaturants on Native-State Structural Fluctuations in Azurin Probed by Molecular Size-Dependent Quenching of Trp Phosphorescence

Giovanni B. Strambini* and Margherita Gonnelli

Consiglio Nazionale delle Ricerche, Istituto di Biofisica, 56124 Pisa, Italy

ABSTRACT: Using azurin as a model protein, this study enquires on the nature of small and large amplitude structural fluctuations permitting the penetration of different size solutes within protein folds, as inferred from quenching of the phosphorescence of buried Trp residues. The work examines the effect that guanidinium hydrochloride and urea have on the migration of a range of quencher molecules of increasing molecular size (M_w range = 32−206 Da). Using the quenching rate constant of Trp phosphorescence as a monitor, the results demonstrate that structural fluctuations linked to O_2 migration are not affected by denaturants, whereas larger amplitude structural fluctuations necessary to facilitate penetration of bulkier quencher molecules [acrylonitrile, acrylamide, *N*-(hydroxymethyl) acrylamide, *N*-[tris(hydroxymethyl) methyl]acrylamide, and 2-acrylamido-2-methyl-1-propanesulfonic acid] are clearly enhanced by the presence of denaturant. These data when interpreted in the context of the amount of new protein surface uncovered to solvent ($\Delta SASA_o$) by the underlying structural fluctuations show a direct correlation between the amplitude of these motions and $\Delta SASA_o$. Denaturants also promote slow frequency (20−80 s^{-1}) conformational transitions, not manifested in normal aqueous solutions, which provide extra migration pathways for acrylamide and its larger derivatives. The quencher-size dependence of the quenching rate provides evidence of multiple, independent quencher migration pathways to the azurin core, which are characterized by motions on different time scales, microseconds and milliseconds, and by a 3- to 5-fold difference in $\Delta SASA_o$, respectively.

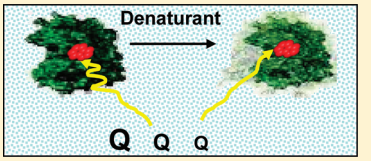

INTRODUCTION

Interest on the dynamic features of protein folds draws from the growing awareness that conformational fluctuations are intimately correlated to biological function. In particular, collective slow motions on a millisecond to microsecond time scale have been directly linked to protein folding,[1,2] enzymatic catalysis, signal transduction, and protein−protein interactions.[3−11] Notwithstanding the relevance to biological function, the frequency−amplitude spectrum of slow motions in globular proteins is still poorly characterized. Indeed, little is known on the intrinsic variability of protein motions among globular folds and on how they are modulated by bound ligands or medium conditions. This scarcity of information is primarily due to the experimental difficulties associated with the characterization of slow motions,[12−15] especially when dealing with transitions to rarely populated conformational substates.

Fluorescence and phosphorescence quenching of buried Trp residues by the diffusive penetration of inert solutes through generally compact globular folds bear direct evidence on the conformational flexibility of the macromolecule. In principle, by varying the quencher (Q) size it should be possible to probe structural fluctuations over a wide range of amplitudes and in a time domain limited only by the emission lifetime. Quenching studies measure the luminescence lifetime (τ) as a function of quencher concentration, [Q], and evaluate the bimolecular quenching rate constant, k_q, from the gradient of the Stern−Volmer plot

$$1/\tau = 1/\tau_0 + k_q[Q] \quad (1)$$

where τ_0 is the unperturbed lifetime. For Trp free in solution and efficient quenching reactions, k_q is close to the diffusion-limited rate constant k_d, where $k_d = 4\pi r_0 D$ (r_0 is the sum of molecular radii and D the sum of the diffusion coefficients). k_q may drop significantly for Trp residues buried within protein folds, the decrease in the rate constant reflecting the extent by which Q migration through the protein matrix is slowed relative to diffusion in water. The technique, initially applied to quenching of Trp fluorescence on the nanosecond time scale,[16] was subsequently extended to the long-lived phosphorescence emission,[17−24] expanding thereby the range of measurable diffusion rates to the second time domain. Recently, the first systematic study on the Q-size (M_w range = 32−206 Da) dependence of k_q compared the permeability of O_2, acrylonitrile, acrylamide, and acrylamide derivatives of increasing molecular weight on four different proteins.[25] The results indicated that, on the millisecond−second phosphorescence time scale, even relatively bulky solutes have access to the internal region of the globular fold, implying that relatively large amplitude structural fluctuations, much more rapid than whole molecule unfolding, are characteristic of native-state dynamics. Only when Trp is deeply buried in compact cores of the macromolecule, as with W48 in azurin or W109 in alkaline phosphatase, is Q migration considerably hindered. Consistent with a penetration mechanism, the quenching rate in these proteins decreases drastically with Q size, k_q dropping 6−7 orders of magnitude from O_2 to acrylamide, while no internal access is permitted to larger acrylamide derivatives. Such strong Q-size discrimination of the quenching rate stands to indicate the sharp rise in free energy

Received: August 31, 2011
Revised: October 12, 2011
Published: October 12, 2011

costs associated with increasing the amplitude of internal motions, presumably reflecting extensive disruption intramolecular of H-bonding networks and exposure of a new protein surface to the solvent (ΔSASA > 0).

Among the most utilized methods for monitoring structural dynamics in proteins are amide hydrogen exchange (HX) reactions[26−30] and more recently pulsed thiol-disulfide (SX) exchange reactions,[31,32] the techniques being specific of backbone and side chain dynamics, respectively. Similarly to luminescence quenching, chemical exchange reactions monitor the rate at which internal target groups, backbone NH, or Cys side chains react with probe reagents (OH^- or disulfides) in the solvent. Chemical exchange processes have been modeled by the Linderström−Lang mechanism in which an opening conformational transition exposes internal target groups to the solvent where exchange takes place

$$\text{Closed} \underset{k_c}{\overset{k_o}{\leftrightarrow}} \text{Open} \xrightarrow{k_{ch}} \text{Exchanged} \qquad (2)$$

where k_o and k_c are the opening and closing rate constants, respectively, and k_{ch} is the reaction rate for solvent exposed groups, which is generally assumed to be equal to the rate constant for exchange from small peptides.[33] Under native conditions, where $k_o \ll k_c$, the rate of exchange is given by[34,35]

$$k_{obs} = k_o k_{ch}/(k_c + k_{ch}) \qquad (3)$$

Conventional HX and SX experiments are conducted in the EX2 regime, $k_c \gg k_{ch}$, where $k_{obs} = K_o k_{ch}$ yields the equilibrium constant $K_o = k_o/k_c$, the free energy change of the opening transition, $\Delta G_o = -RT \ln K_o$, and from the dependence of ΔG_o on the denaturant concentration its m value.[28] On the basis of the dependence of the exchange rate on the denaturant concentration, opening transitions have been classified as local structural fluctuations, or breathing motions, and subglobal unfolding and global unfolding events. Local structural fluctuations are insensitive to the denaturant implying that little surface area ($\Delta SASA_o$) is uncovered in these transitions. Apparently, most backbone amides and buried Cys residues can exchange by way of local structural fluctuations,[28,31,36] suggesting that the formation of exchange competent open conformers requires little disruption of the native-state fold even when it involves deeply buried sites or bulky disulfide reagents (up to nearly 400 in M_w[31]). Yet, the ΔG_o values estimated for these light transitions often approach ΔG for whole molecule unfolding, an apparent paradox that has been pointed out before.[37,38] Concerns have been raised on the universal applicability of eq 2 as well as on the actual magnitude of k_{ch}, which can be markedly affected by the local chemical reactivity or hydrogen bonding network.

To provide an independent view on the nature of small and large amplitude structural fluctuations in proteins, this study examines the effect of classical denaturants, guanidinium hydrochloride (Gdn), and urea on the quenching rate constant (k_q) of solutes of various molecular size (M_w range = 32 −206 Da), using azurin as a model protein system. Azurin is a 14 kDa copper protein containing a single Trp residue (W48) located in the central core of the globular fold, well removed from the aqueous interface[39] to be shielded from trivial quenching by Q in the solvent. The C112S mutant is unable to bind Cu and displays strong and long-lived Trp phosphorescence at ambient temperature (τ_0 = 0.44 s at 20 °C). The protein undergoes reversible denaturation, and both equilibrium and kinetics of unfolding have been characterized in detail as a function of [Gdn].[40] In this study, quenching profiles were obtained for each quencher of Figure 1, at two or three predenaturation concentrations of Gdn and one concentration of urea, at both −5 and 25 °C. The results indicate that whereas the denaturant has a negligible influence on the small-amplitude fluctuations implicated in the migration of O_2 it progressively enhances the internal diffusion of bigger solutes indicating that larger amplitude motions are characterized by sizable $\Delta SASA_o$.

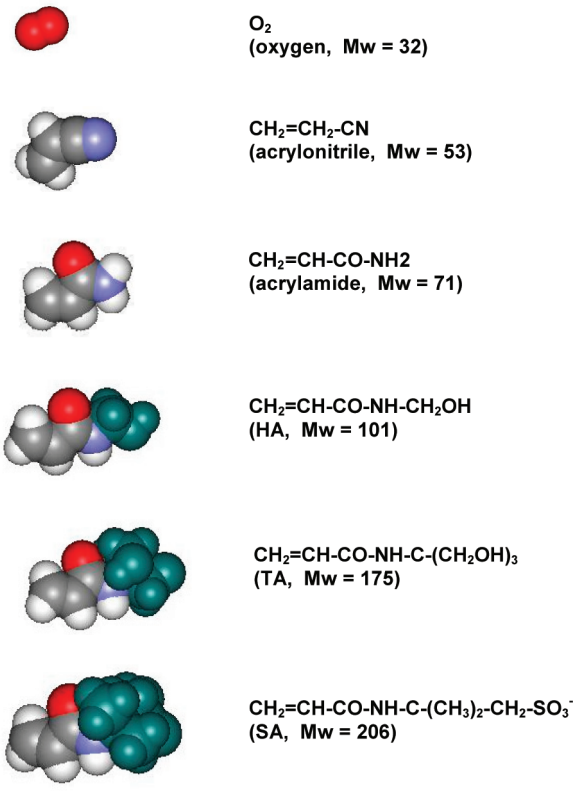

Figure 1. Space filling model and chemical formula of quenching solutes considered in this study.

EXPERIMENTAL METHODS

All chemicals were of the highest purity grade available from commercial sources and unless specified to the contrary were used without further purification. Acrylamide (99.9% electrophoretic purity) was from Bio-Rad Laboratories (Richmond, CA). *N*-(Hydroxymethyl) acrylamide (HA) (>98%) was from TCI Europe (Zwijndrecht, Belgium). Acrylonitrile (AN) (99%), *N*-[tris(hydroxymethyl)methyl]acrylamide (TA) (93%), and 2-acrylamido-2-methyl-1-propanesulfonic acid sodium salt (SA) were from Sigma-Aldrich (Italy). Enzyme grade urea and guanidine HCl were from USB Corporation (Cleveland, OH). Tris-(hydroxymethyl)-aminomethane (Tris) and NaCl Suprapur were from Merck (Darmstadt, Germany). Water was purified by reverse osmosis (Milli-RX 20; Millipore, Billerica, MA) and subsequently passed through a Milli-Q Plus system (Millipore Corporation, Bedford, MA). The mutant C112S of azurin from *Pseudomonas aeruginosa* was prepared following a procedure analogous to that described by Karlsson et al.,[41] using the QuikChange kit (Stratagene, La Jolla, CA) and confirmed by sequencing.

Phosphorescence Measurements. For phosphorescence measurements in fluid aqueous solutions, protein samples, 6 μM in concentration, were placed in oppositely constructed, 5 × 5 mm^2, quartz cuvettes with a leak-proof capping designed to allow thorough removal of O_2 by the alternating application of moderate vacuum and inlet of ultrapure N_2.[42] Only in experiments with AN, which is moderately volatile and in which the application of N_2 flushing/vacuum would reduce the AN concentration in solution, sample deoxygenation was carried out by the enzymatic system.[43] Enzymatic O_2 removal was found to be efficient also in the presence of denaturants indicating that under the present experimental conditions the enzyme couple remains active.

Phosphorescence spectra and decays were measured with pulsed excitation on a homemade apparatus.[23,42] The exciting light (λ_{ex} = 292 nm) was provided by a frequency-doubled Nd/Yag-pumped dye laser (Quanta Systems, Milano, Italy) with pulse duration of 5 ns and a typical energy per pulse around 0.05 mJ. For decay measurements, the phosphorescence intensity was collected at 90° from vertical excitation through a filter combination with a transmission window of 405−445 nm (WG405, Lot-Oriel, Milano Italy, plus interference filter DT-Blau, Balzer, Milano, Italy) and monitored by a photomultiplier (EMI 9235QA, Middlesex, UK). The prompt Trp fluorescence intensity from the same pulse was also recorded and used to account for possible variations in the laser output as well as to obtain fluorescence-normalized phosphorescence intensities. A decrease in the latter occurs when there is partial quenching of phosphorescence during the dead time of these measurements, as for example in the case of static interaction with closely bound quenchers. All phosphorescence decays could be adequately fitted to a single exponential component by a nonlinear least-squares fitting algorithm (DAS6, Fluorescence decay analysis software, Horiba Jobin Yvon, Milano, Italy).

Quenching Experiments. Quenching experiments measure the phosphorescence lifetime, τ, of protein samples as a function of the quencher concentration [Q] in solutions and derive the bimolecular quenching rate constant, k_q, from the gradient of the Stern−Volmer plot (eq 1). Fitting of quenching rates to theoretical models was carried out with the program Origin.

Acrylonitrile, acrylamide, and acrylamide derivative stock solutions were prepared daily by diluting commercial supplies in the appropriate denaturant/buffer (30 mm Tris, pH 7)/azurin solution. To take into account the increase in ionic strength of Gdn solutions, blank tests were carried out in which the denaturant was replaced by equimolar KCl. In general [Q] ≤ 1 M, the maximum concentration dictated by either the solubility of Q or the lifetime resolution of the apparatus (quenching rates ≤6 × 10^4 s^{-1}). For each quencher concentration, at least three independent samples were analyzed, and the reported results represent the mean lifetime value. The reproducibility of phosphorescence lifetime measurements was generally better than 7%. With O_2 quenching, the highest concentration employed was that of an aqueous solution in equilibrium with the atmosphere, as derived from the solubility of O_2 (258 μM at 25 °C). Smaller O_2 concentrations obtained by partial degassing were determined directly from the lifetime of alkaline phosphatase (1.3 μM) added to the azurin sample, as described before.[44]

Quenching Models. For buried Trp residues, quenching of phosphorescence by small solutes (Q) in solution is generally analyzed in terms of mechanisms that involve either Q diffusion to the protein surface followed by long-range interactions with the buried chromophore (external quenching) or diffusive Q penetration of the protein matrix to the proximity of the chromophore. Pertinent analytical expressions for the quenching rate, obtained by solving Fick's diffusion equation applying radiation boundary conditions, and their application range in the realm of protein phosphorescence have been discussed in detail before.[45] Briefly, by neglecting a transient time-dependent term arising from Q molecules already in proximity of the chromophore at the instant of excitation, the steady state bimolecular quenching rate constant, k_q, is given by

$$k_q = k_D k_I/(k_D + k_I) \quad (4)$$

where $k_D = 4\pi aD$ is the Smoluchowski diffusion-controlled rate constant; $k_I = 4\pi a^2 B$ is the diffusion-independent maximum rate constant; and D is the sum of the separate diffusion coefficients of Q and protein in solution. B is an interaction strength parameter related to the distance dependence of the quenching interaction, $k(r)$, and a is the distance (center-to-center) of closest approach between Q and the chromophore. Depending on which of the two rate constants is smaller, the process goes from the diffusion-controlled regime ($k_D \ll k_I$, $k_q = k_D \propto D$) to the reaction-controlled regime ($k_D \gg k_I$, $k_q = k_I$), where k_q is independent of diffusion.

External quenching of protein phosphorescence by freely diffusing Q relegated to the aqueous phase was recently shown to rigorously comply with the rapid diffusion limit (RDL) regime.[46] The bimolecular rate constant, k_I(RDL), derived for an essentially flat protein surface and an exponential distance dependence of the interaction {$k(r) = k_0 \exp[-(r - r_0)/r_e]$, r_0 is the center to center distance between Q and the chromophore in van der Waal's contact} decreases with the thickness of the protein spacer (r_p) separating the chromophore from the aqueous interface ($r_p = r - r_0$, r is the shortest center-to-center distance between the internal chromophore and Q at the aqueous interface) according to[47]

$$k_I(\mathrm{RDL}) = k_I(r_p) = 2\pi N 10^{-3}[(r_p + r_0){r_e}^2 + 2{r_e}^3]k_0 \exp(-r_p/r_e)\ \mathrm{M}^{-1}\ \mathrm{s}^{-1} \quad (5)$$

where N is Avogadro's number and r_e is the attenuation length (units of r_e and r_p in cm). For acrylamide, k_0 = 3.5 × 10^{10} M^{-1} s^{-1}; r_e = 0.29 Å; and r_0 = 5 Å.[46] Equation 5 is useful for estimating the possible contribution of external quenching to the overall quenching rate of acrylamide and its larger derivatives.

Penetration of the globular fold by solutes requires fluctuations in the compact structure creating temporary internal cavities or channels to the solvent. For small molecules like O_2 that move rapidly through protein matrices, migration is generally pictured as a random walk process in which Q jumps between "solvation" cages (protein cages). In this scenario, k_q is conveniently expressed in the language of bulk diffusion through a homogeneous protein phase by means of a corrected Smoluchowski equation[45,48]

$$k_q(\mathrm{diffusion}) = 4\pi a D_p(1 + a/T) \quad (6)$$

where $D_p \ll D$ is the diffusion coefficient of Q within a permeable protein shell of thickness T and a is the radius of the impermeable protein core surrounding the chromophore. For bulky Q's, such as acrylamide and its larger derivatives, internal migration will require conformational transitions opening a channel (protein gate) to the buried chromophore (a process similar to that modeled by eq 2). Protein-gated Q access gives rise to a hyperbolic Stern−Volmer plot in which the quenching rate constant k_q(gate) is

described by[23]

$$k_q(\text{gate}) = k_o k_{qo}/(k_c + k_{qo}[Q]) = k_o/(\sigma + [Q]) \quad (7)$$

where k_o and k_c are the gate opening and closing rates, respectively. $k_{qo}[Q]$ represents the quenching rate of the protein in the "open-gate" configuration, and $\sigma = k_c/k_{qo}$ is the Q concentration at midpoint saturation of the protein gate. At large [Q], in the limit $k_c \ll k_{qo}[Q]$, the reaction falls under the EX1 regime, and the rate becomes limited by the gate-opening frequency k_o (is independent of the quencher concentration)

$$k_q(\text{gate})[Q] = k_o \quad (8)$$

At the other extreme, in the low [Q] end where $k_c \gg k_{qo}[Q]$, the reaction falls under the EX2 regime, and the rate constant becomes

$$k_q(\text{gate}) = k_o/\sigma = (k_o/k_c)k_{qo} = K_o k_{qo} \quad (9)$$

where K_o is the opening equilibrium constant. Note that within the EX2 regime the quenching rate is linear with [Q], and therefore experiment cannot distinguish between eqs 9 and 6, which represent alternative but equivalent description (molecular and bulk level, respectively) of the reaction.

In principle, an additional contribution to quenching may come from Q binding to the protein surface (rapid and reversible binding with a dissociation constant K_d)[23]

$$k_q(\text{binding}) = k(r')/([Q] + K_d) \quad (10)$$

where $k(r')$ is the quenching rate of Q bound at a distance r' from the chromophore. We will argue in the Discussion section that for deeply buried W48 of azurin superficial binding of acrylamide or its derivatives will make negligible contribution to the quenching rate.

Downward curving Stern–Volmer plots were fitted to a general expression that includes both diffusive and protein-gated Q migration

$$k_q[Q] = (k_{ql} + k_o/(\sigma + [Q]))[Q] \quad (11)$$

yielding the parameters k_{ql}, k_o, and σ. k_{ql} represents the linear component of the quenching rate and in principle is the sum of contributions from diffusive type Q migration (eqs 6 and 9) as well as spurious external quenching (eq 5), which may often be distinguished from the former by a significantly different dependence on temperature.

RESULTS

Quenching experiments were carried out at selected Gdn concentrations up to 1.3 M and at 4 M urea, above which the protein rapidly unfolds. The chosen temperatures are 25 and −5 °C, undercooled solutions permitting to expand the temperature range of phosphorescence measurements below ambient temperature, where they are less problematic (longer lifetimes and less undesirable spurious contributions) than at higher temperature. To take into account possible effects on the quenching rate due to the increase of the ionic strength in Gdn solutions, control quenching experiments were also carried out in equimolar concentrations of KCl. At the highest denaturant concentrations, the fluorescence spectrum indicated that typically 80–90% of the protein is native ($[D]_{50\%}$ is 1.5 7 M Gdn[40]and 4.7 M in urea), although the unfolded fraction almost doubled when 4 M urea samples were brought to −5 °C, indicating that urea is a more effective denaturant at −5 °C than

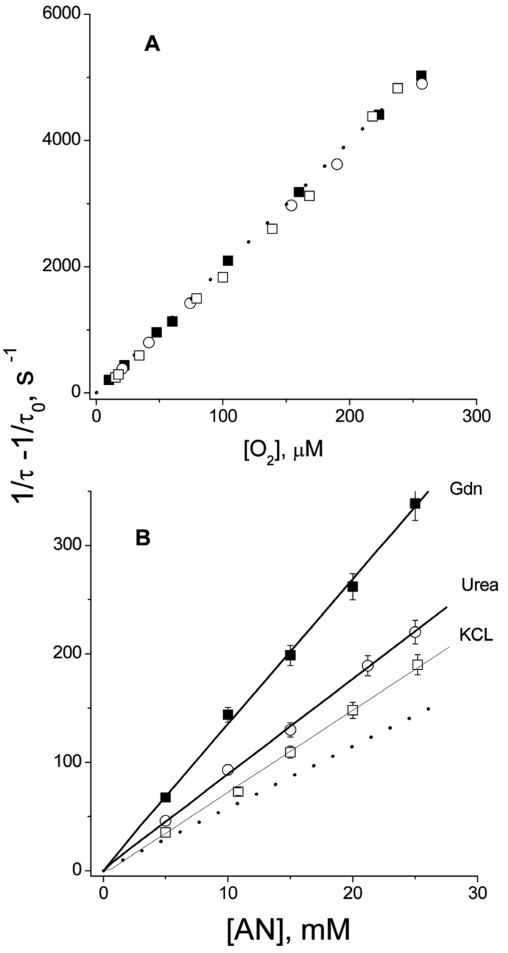

Figure 2. Effect of Gdn and urea on the lifetime Stern–Volmer plots relative to quenching of C112S azurin phosphorescence by O_2 (panel A) and acrylonitrile (panel B), at 25 °C: (□) 1.3 M KCl; (■) 1.3 M Gdn; (○) 4 M urea. The dotted line refers to buffer (30 mM Tris, pH 7). Full lines are linear fits of the data.

at 25 °C. In general, the unfolded fraction remained invariant upon the addition of quenching reagents, suggesting that even at their highest concentration (≈ 0.8 M) these compounds do not significantly affect the stability of azurin. It should be noted that, even under denaturing conditions, quenching experiments report selectively on the Q accessibility to the native fold, as the unfolded protein is not phosphorescent (at $[D]_{50\%}$ the lifetime drops from 140 to 150 ms of the native protein to submilliseconds for the denatured state). Both Gdn and urea have a moderate effect on the native-state lifetime, the reduction of τ_0 from 240 ms in buffer to 155 ms in 1.3 M Gdn and to 163 ms in 4 M urea presumably reflecting a denaturant-induced weakening of the tertiary structure, although the reduction of τ_0 could partly be due to spurious quenching from trace impurities in commercial denaturant stocks.

O_2 Quenching. O_2 quenching was measured only in 1.3 M Gdn and in 4 M urea, at 25 °C. The highest concentration employed was that of an aqueous solution in equilibrium with the atmosphere. Smaller concentrations, obtained by partial degassing, were determined using the protein alkaline phosphatase (AP) as an internal monitor of the O_2 activity,[44] after verifying that the O_2 permeability of AP is not altered by the denaturants. Indeed, based on measurements on air equilibrated solutions (O_2 activity = 258 μM at 25 °C), the value for $k_q(O_2)$ of AP ($k_q[O_2] = 1/\tau - 1/\tau_0$)

Table 1. Effect of Gdn and Urea on the Parameters Describing the Quenching Rate Constant of C112S Azurin Phosphorescence Relative to Solutes Q of Increasing Molecular Size

Q	D, [ ]	k_o (s^{-1})	σ (M)	k_o/σ (M^{-1} s^{-1})	k_{ql} (M^{-1} s^{-1})
			T = 25/−5 °C		
O_2	buffer				2.0 ± 0.06E7
"	KCl, 1.3				1.88 ± 0.1E7
"	Gdn, 1.3				0.97 ± 0.08E7
"	urea, 4				1.84 ± 0.09E7
AN	buffer				5.70 ± 0.2E3 /400 ± 33
"	KCl, 1.3				7.56 ± 0.3E3 /517 ± 30
"	Gdn, 1.3				1.33 ± 0.1E4 /980 ± 74
"	urea, 4				8.70 ± 0.4E3 /870 ± 84
acryl	buffer				66 ± 4/ 2.4 ± 1.3
"	KCl, 0.6				78 ± 6/ 2.9 ± 0.5
"	KCl, 1.0				83 ± 6/ 3.2 ± 1.5
"	KCl, 1.3				104 ± 5/ 3.6 ± 2.1
"	Gdn, 0.6	54 ± 9/ 3.8 ± 0.4	0.17 ± 0.06/ 0.27 ± 0.06	318/14	110 ± 7/ 3.7 ± 1.5
"	Gdn, 1.0	74.3 ± 12/ 4.4 ± 0.3	0.097 ± 0.03/ 0.14 ± 0.1	766/31	172 ± 11/ 7.0 ± 2.1
"	Gdn, 1.3	77.5 ± 18/ 5.7 ± 0.4	0.052 ± 0.01/ 0.05 ± 0.007	1490/114	271 ± 15/ 9.7 ± 1.8
"	urea, 4	63 ± 14/ 6.5 ± 1.6	0.18 ± 0.1/ 0.27 ± 0.09	350/24	140 ± 9/ 7.0 ± 2.2
HA	buffer				25 ± 3/ 1.3 ± 0.5
"	KCl, 0.5				27 ± 2/ 1.3 ± 0.7
"	KCl, 0.9				29 ± 3/ 1.5 ± 0.5
"	KCl, 1.3				34.5 ± 4/ 1.6 ± 0.4
"	Gdn, 0.5	21.0 ± 5/----	0.21 ± 0.06/-----	100/----	36 ± 4/ 2.4 ± 0.8
"	Gdn, 0.9	36.0 ± 4/ 1.4 ± 0.2	0.10 ± 0.04/ 0.10 ± 0.05	360/14	47 ± 11/ 2.4 ± 0.3
"	Gdn, 1.3	60.3 ± 9/ 2.8 ± 1.5	0.08 ± 0.03/ 0.087 ± 0.06	753/32	68 ± 10/ 3.1 ± 1.0
"	urea, 4	49 ± 11/ 3.6 ± 1.5	0.12 ± 0.01/ 0.06 ± 0.04	408/60	52 ± 8/ 3.6 ± 1.6
TA	buffer				11 ± 3/ 2.3 ± 1.1
"	KCl, 1.3				10 ± 2/ 1.9 ± 1.3
"	Gdn, 0.8	15.5 ± 3/ 1.2 ± 0.05	0.12 ± 0.02/ 0.13 ± 0.02	129/9	8 ± 2/ 1.0 ± 1.1
"	Gdn, 1.3	32.1 ± 5/ 2.3 ± 0.2	0.11 ± 0.02/ 0.03 ± 0.01	292/77	10 ± 3/ 1.1 ± 1.6
"	urea, 4	19.4 ± 4/ 1.5 ± 0.17	0.091 ± 0.03/ 0.08 ± 0.02	213/19	10 ± 1/ 1.6 ± 1.8
SA	buffer				9.4 ± 3/ 4.5 ± 2.0
"	KCl. 1.3				11.5 ± 2/ 5.0 ± 1.5
"	Gdn, 0.8	10 ± 0.65/ 1.6 ± 0.52	0.14 ± 0.03/ 0.117 ± 0.027	71/13.6	10.1 ± 2/ 2.6 ± 1.2
"	Gdn, 1.3	24.2 ± 1/ 2.2 ± 0.96	0.125 ± 0.02/ 0.097 ± 0.04	194/22.7	8.0 ± 3/ 3.0 ± 1.6
"	urea, 4	13.7 ± 3.5/ 1.0 ± 0.5	0.097 ± 0.04/ 0.04 ± 0.02	141/25	9.1 ± 3.8/ 3.2 ± 2.1

was 1.63 ± 0.06 × 10^6 M^{-1} s^{-1} in 1.3 M KCl, 1.47 ± 0.05 × 10^6 M^{-1} s^{-1} in 1.3 M Gdn, and 1.62 ± 0.07 × 10^6 M^{-1} s^{-1} in 4 M urea. These values are not significantly different from 1.65 ± 0.04 × 10^6 M^{-1} s^{-1} measured in buffer and indicate that the O_2 permeability of AP is not markedly affected by either the denaturant or the increase in ionic strength of the solution.

O_2 quenching of azurin in the presence of denaturants exhibits linear Stern−Volmer plots (Figure 2A) yielding quenching rate constants equal to 1.88 ± 0.1 × 10^7 M^{-1} s^{-1} in 1.3 M KCl, 1.97 ± 0.08 × 10^7 M^{-1} s^{-1} in 1.3 M Gdn, and 1.84 ± 0.09 × 10^7 M^{-1} s^{-1} in 4 M urea. In all cases, a value practically indistinguishable from 2.0 × 10^7 M^{-1} s^{-1} obtained in buffer. Thus, at these concentrations of Gdn and urea the permeability of the azurin core to O_2 is practically the same as in buffer.

AN Quenching. Quenching by acrylonitrile was examined in 1.3 M Gdn and 4 M urea, at 25 and −5 °C. The implementation of enzymatic O_2 removal introduced a phosphorescence component from the enzymatic system that decayed during the initial 1−2 ms, limiting thereby the range of detectable quenching rate to k_q[AN] < 500 s^{-1}.

In both Gdn and urea solutions, the Stern−Volmer plots are essentially linear on [AN] (Figure 2B). The rate constant derived from the slope (Table 1) indicates that, relative to buffer, AN quenching is over 2-fold more efficient in 1.3 M Gdn and about 50% more efficient in 4 M urea. The 1.3 M KCl control revealed, however, that the greater increase of k_q in Gdn, in comparison to urea, may be partly due to the concomitant increase in ionic strength. When k_q is normalized by a reference state at the same ionic strength, the rate enhancement by the denaturant (the factor R in Table 2) amounts to 76% for 1.3 M Gdn and 53% for 4 M urea.

From 25 to −5 °C, k_q drops by over 10-fold. At the lower temperature, the rate enhancement by the denaturant is substantially unchanged in Gdn but becomes twice as large as that at 25 °C in urea (Table 1), which may be related to the enhanced denaturing efficacy of the latter at −5 °C. From the temperature

Table 2. Denaturant-Induced Enhancement of k_{ql} (R) and Activation Enthalpies ($\Delta H^{\pm}$) Relative to k_{ql} and k_o (from Data of Table 1)

Q	D, []	R^a	$\Delta H^{\pm}(k_o)$ (kcal mol^{-1})	$\Delta H^{\pm}(k_{ql})$ (kcal mol^{-1})
		T = 25/−5 °C		
O_2	buffer			9.4[b]
"	KCl, 1.3			
"	Gdn, 1.3	≈1		
"	urea, 4	≈1		
AN	buffer			14.1
"	KCl, 1.3			14.2
"	Gdn, 1.3	1.76/1.89		13.8
"	urea, 4	1.53/2.17		12.2
acryl	buffer			17.6
"	KCl, 0.6			17.1
"	KCl, 1.0			17.2
"	KCl, 1.3			17.8
"	Gdn, 0.6	1.4/1.3	14.1	18.0
"	Gdn, 1.0	2.07/2.2	15.0	17.0
"	Gdn, 1.3	2.6/2.7	15.2	17.6
"	urea, 4	2.1/2.9	12.0	15.9
HA	buffer			15.7
"	KCl, 0.5			16.1
"	KCl, 0.9			15.7
"	KCl, 1.3			16.3
"	Gdn, 0.5	1.3/1.6		14.3
"	Gdn, 0.9	1.5/1.6	17.2	15.8
"	Gdn, 1.3	1.9/1.9	16.3	16.4
"	urea, 4	2.08/2.8	13.9	14.1
TA	buffer			8.3
"	KCl, 1.3			8.8
"	Gdn, 0.8	≈1	13.4	11.0
"	Gdn, 1.3	≈1	14.0	11.7
"	urea, 4	≈1	13.6	9.7
SA	buffer			3.9
"	KCl. 1.3			4.4
"	Gdn, 0.8	≈1	9.7	7.2
"	Gdn, 1.3	≈1	14.0	5.2
"	urea, 4	≈1	13.6	5.5

[a] $R = k_{ql}$(denaturant)/k_{ql}(control). [b] From ref 25.

dependence of k_q, $[\ln(k_q(T_1)/k_q(T_2)) = \Delta H^{\pm}(k_q)/R(1/T_2 - 1/T_1)]$, we may infer an activation enthalpy for AN migration, $\Delta H^{\pm}(k_q)$, of about 14 kcal mol^{-1}, practically the same in buffer, KCl, and Gdn solutions, and of about 2 kcal mol^{-1} smaller in urea.

Acrylamide Quenching. Both denaturants distinctly enhanced the acrylamide quenching rate, although they also introduced a markedly nonlinear dependence of the rate on [acrylamide], as illustrated by downward-curving Stern−Volmer plots (Figure 3). Experiments were carried out at three Gdn concentrations (0.6, 1.0, and 1.3 M), together with isotonic KCl blanks, and in 4 M urea. The quenching profiles of Figure 3 show a progressive increase of the quenching rate with Gdn concentration, the enhancement being invariably associated to nonlinear Stern−Volmer plots. KCl blanks confirm a moderate effect of ionic strength on the quenching rate, although under these conditions the plot remained linear with

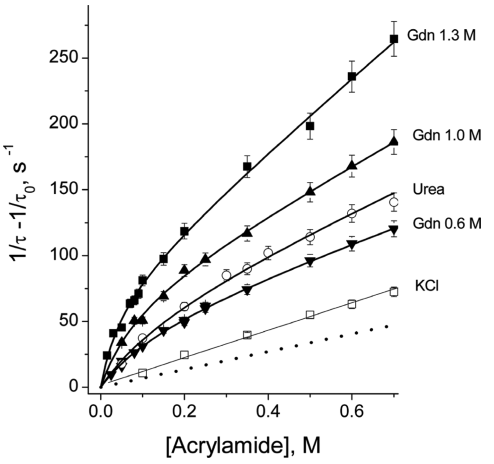

Figure 3. Effect of Gdn and urea on the lifetime Stern−Volmer plots relative to quenching of C112S azurin phosphorescence by acrylamide, at 25 °C: (□) 1.3 M KCl; (■) 1.3 M Gdn; (▲) 1.0 M Gdn; (▼) 0.6 M Gdn; (○) 4 M urea. The dotted line refers to buffer (30 mM Tris, pH 7). The thick full lines represent fits of the data to a single-gate model (eq 5) plus a linear component {rate = k_q[Q] = $(k_o/(\sigma + [Q]) + k_{ql})$[Q]}.

[acrylamide]. Downward-curving Stern−Volmer plots have been reported previously with quenching of alcohol dehydrogenase phosphorescence by acrylamide and larger derivatives,[23,25] and this unusual behavior was attributed to saturating, protein-gated quencher penetration (eq 7). All quenching profiles of Figure 3 were adequately fitted utilizing a single-gate model plus a linear component (eq 11). According to this analysis, in the presence of either denaturant, the data discern at least two independent migration pathways: one involving relatively slow protein-gated Q penetration that tends to saturate at submolar Q concentrations and the other engaging more rapid protein motions permitting diffusive-like Q migration. The latter pathway, represented by the rate constant k_{ql}, is presumably the same migration route of acrylamide in the absence of denaturant. As indicated in Table 1 Gdn enhances significantly diffusive migration of acrylamide (k_{ql} increasing up to 2.6-fold relative to the isotonic control), while it also promotes an independent access route to the site of W48, or to its proximity, involving structural fluctuations in the frequency (k_o) range 50−80 s^{-1}. With regard to the latter pathway the gate opening frequency (k_o) increases moderately, from 50 to 80 s^{-1}, from 0.6 to 1.3 M Gdn, whereas the saturation midpoint (σ) decreases by over 3-fold, from 170 to 52 mM. If it is assumed that the "open-gate" quenching rate constant, k_{qo}, is independent of [Gdn], namely, that the structure of the open protein conformer is not altered by the denaturant, then the decrease of $\sigma = k_c/k_{qo}$ would essentially reflect a reduction of the gate closing frequency k_c. Likewise, the progressive increase in the parameter $k_o/\sigma = (k_o/k_c)k_{qo}$ (Table 1) at higher Gdn concentrations would simply be a consequence of the stabilization of the open-gate conformation ($K_o = k_o/k_c$) by the denaturant. The data obtained in 4 M urea give evidence of a similar action by the neutral denaturant, suggesting that the above enhancement of the quenching rate is a characteristic of solvents that promote protein unfolding, rather than being the result of peculiar protein−Gdn interactions.

Upon lowering the temperature to −5 °C, the quenching reaction is significantly slowed down, but the denaturant-induced enhancements and the curvature of Stern−Volmer plots are

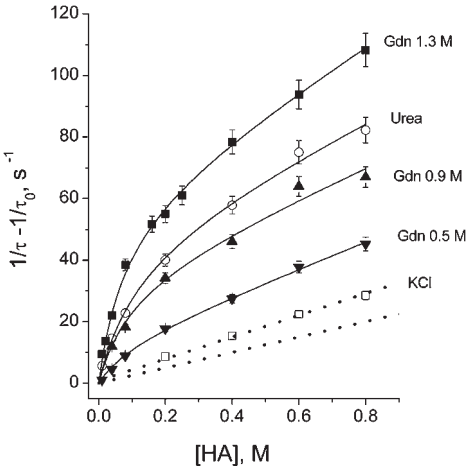

Figure 4. Effect of Gdn and urea on the lifetime Stern−Volmer plots relative to quenching of C112S azurin phosphorescence by HA, at 25 °C: (□) 1.3 M KCl; (■) 1.3 M Gdn; (▲) 0.9 M Gdn; (▼) 0.5 M Gdn; (○) 4 M urea. The dotted line refers to buffer (30 mM Tris, pH 7). The thick full lines represent fits of the data to a single-gate model plus a linear component.

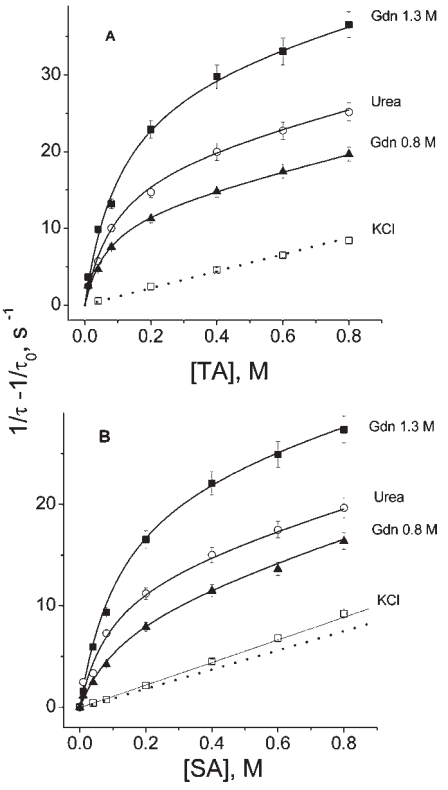

Figure 5. Effect of Gdn and urea on the lifetime Stern−Volmer plots relative to quenching of C112S azurin phosphorescence by TA (panel A) and SA (panel B), at 25 °C: (□) 1.3 M KCl; (■) 1.3 M Gdn; (▲) 0.8 M Gdn; (○) 4 M urea. The dotted line refers to buffer (30 mM Tris, 850 mM KCl, pH 7). The thick full lines represent fits of the data to a single-gate model plus a linear component.

analogous to those observed at 25 °C. In fact, the plots at −5 °C are equally well fitted in terms of a single-gate model plus a linear component. The main effect of lowering the temperature, as indicated in Table 1, is an over 10-fold reduction of both the constant k_{ql} and the gate frequency k_o. As noted above with AN, the drop in quenching efficiency at −5 °C is less marked in urea than in Gdn (Table 1). The activation enthalpies, $\Delta H^{\pm}(k_{ql})$ and $\Delta H^{\pm}(k_o)$ (Table 2), estimated from two-point Arrhenius plots fall in the 17−18 kcal mol^{-1} range for k_{ql} (the same value observed in buffer) and in the 12−15 kcal mol^{-1} range for k_o, respectively, with no significant influence of the denaturant on the activation barriers. It is interesting to note that the value of $\Delta H^{\pm}(k_{ql})$ increases steadily from O_2 to AN and to acrylamide indicating that the activation barrier to Q diffusion increases with the amplitude of the underlying structural fluctuations.

HA Quenching. Among the quenchers examined here, HA is the largest molecule capable of quenching azurin phosphorescence in buffer. With the addition of denaturant, from 0.5 to 1.3 M Gdn, or 4 M urea, the reaction becomes noticeably more rapid although, like for acrylamide, the Stern−Volmer plot becomes highly nonlinear on [HA], exhibiting marked saturation at [HA] above 100 mM Figure 4). Throughout, the data were satisfactorily fitted by a single-gate model plus a linear component (k_{ql}), and the fitting parameters are collected in Table 1. In Gdn, k_{ql} increases up to 2-fold relative to the corresponding controls, while the gate frequency k_o, which is smaller relative to the putative acrylamide gate and more sensitive to the denaturant concentration, increases from 21 to 60 s^{-1}. The corresponding value of σ is in the 100 mM range and decreases progressively from 210 to 80 mM. As before, by assuming that the nature of the "open state", and therefore the magnitude of k_{qo}, is invariant from 0.5 to 1.3 M Gdn, we would infer that from 0.5 to 1.3 M Gdn k_c decreases 2.5-fold, while K_o increases 7.5-fold. The results in 4 M urea are fully consistent with the data obtained in Gdn (k_o = 49 s^{-1} and σ = 120 mM).

At −5 °C, both the gate frequency and the linear quenching component are considerably slowed down. In 0.5 M Gdn, the quenching enhancement is so modest that a linear fit of the Stern−Volmer plot is equally satisfactory as a single-gate fit. As noted with the other quenchers, the temperature-induced drop in quenching efficiency is less in urea than in Gdn. The estimated activation barrier is in the 14−16 kcal mol^{-1} range for k_{ql} and in the 14−17 kcal mol^{-1} range for k_o, respectively. Smaller values generally refer to urea solutions.

TA and SA Quenching. We recall that the two largest acrylamide derivatives, TA and SA, are apparently unable to penetrate the azurin fold in the second time scale even if a slight quenching is also detected from these compounds (k_{ql} = 9.5−11 M^{-1} s^{-1} at 25 °C). However, the small activation enthalpy, ≤ 10 kcal mol^{-1}, associated with it is not consistent with large amplitude structural fluctuations permitting Q penetration.[25] Such residual quenching has been attributed to spurious reactions with moieties in the solvent, either additives that block Q polymerization or impurities in commercial Q supplies.

With TA and SA, the reference state "buffer" refers to solutions at a constant ionic strength of 880 mM, which permits us to compensate for ionic strength variations introduced by SA, which is a charged molecule, and by TA whose supply contains 7% KCl. The denaturant concentrations were 0.8 and 1.3 M Gdn and 4 M urea with TA and 1.3 M Gdn and 4 M urea with SA. Both Gdn and urea enhanced significantly the quenching rate of TA and SA. In all cases the denaturant gave rise to highly nonlinear Stern−Volmer plots, which were adequately fitted by a single-gate plus a linear component model (Figure 5). The fitting parameters, collected in Table 1, point out that denaturant-induced quenching is due entirely to protein-gated Q penetration as there is

practically no influence of the denaturant on the linear component (k_{ql} = 9−10 M^{-1} s^{-1} as in buffer). The invariance of k_{ql}, despite the greater conformational flexibility of azurin in the presence of denaturant, is fully consistent with the assignment of the linear component to external quenching by impurities. The results indicate a decrease of the gate frequency with Q size, from 32 s^{-1} of TA to 22 s^{-1} of SA (in 1.3 M Gdn) and from 19 to 14 s^{-1}, in 4 M urea, respectively, while σ falls within the 70−110 mM range, throughout.

At −5 °C, quenching by TA and SA is considerably slowed down, approaching the limit of detection, and although the denaturant enhancement and the non linearity of the rate are clearly manifest, the uncertainty in the fitting parameters is amplified by the modest effects. At lower temperature, the gate frequency is reduced to the 1−2 s^{-1} range and is associated to an activation barrier, $\Delta H^{\ddagger}(k_o)$, of 10−14 kcal mol^{-1}. Again, no denaturant effects are observed on the linear component.

DISCUSSION

Quenching rate constants have been interpreted in terms of structural fluctuations in the native fold of azurin that permit Q access to internal W48. The assumption is that contributions from long-range through-space interactions with Q in the solvent (eq 5) or bound to the protein surface (eq 10) are negligible, a concern with big acrylamide derivatives for which diffusive migration could be highly hindered. These alternative quenching mechanisms are amply ruled out by the following considerations. For a random Q distribution in the solvent, external quenching can be estimated applying eq 5, $k_I(r_p)$, whose validity has recently been experimentally confirmed.[46] According to the protein crystallographic structure,[39] W48 is separated from the aqueous interface by a distance $r_p \geq 0.8$ nm, which yields $k_I(r_p) \leq 1.5 \times 10^{-4}$ M^{-1} s^{-1} for acrylamide and even smaller values for the larger derivatives, implying that the interaction with Q in the solvent is well out of range. External quenching can become more efficient if Q binds to the protein surface, in which case the corresponding Stern−Volmer plot would assume the form of a hyperbolic binding curve (eq 10). Such a behavior was indeed observed with acrylamide and its larger derivatives, even if only in the presence of denaturant. We have interpreted the curvature in these profiles in terms of protein-gated Q penetration (eq 7) because the alternative binding mechanism (eq 10) cannot account for the magnitude of k_q. According to eq 10, the maximum quenching rate by Q bound at a distance r' from the chromophore is $k_q(\text{binding})[Q] \leq k(r')$. Even considering the closest possible binding site on the azurin surface ($r' \geq 0.8$ nm), we obtain $k(r') \leq 0.03$ s^{-1}, which is at least 100-fold smaller than experimental values (the value of k_o in Table 1). Furthermore, binding affinity (K_d) being specific of Q structure and charge would be expected to exhibit a great variability among the acrylamide derivatives, which is not observed here (see σ values of Table 1). The assignment of the nonlinear component to protein-gated quencher penetration (eq 7) is also supported by an invariably large, ≈15 kcal mol^{-1}, activation barrier for k_o, a value about 3 times larger than the 5 kcal mol^{-1} typically associated with $k(r)$ of the acrylamide moiety.[46]

This study enquires on native-state structural fluctuations in azurin that occur on a time scale shorter than τ_0 (≈200 ms) and in a range of amplitudes that permit the access to the protein core of solutes of M_w from 32 to 206 Da. The sharp, exponential drop of the quenching rate constant with Q size (k_q drops about 6 orders of magnitude from O_2 to HA, M_W = 32−101 Da, becoming undetectably small with larger acrylamide derivatives) and the progressive increase in the activation barrier of the quenching rate emphasize the steep rise in free energy costs associated with larger amplitude motions in azurin. Denaturants, by stabilizing partly unfolded "open" conformers, are expected to promote transitions that involve significant exposure of protein surface area to the solvent ($\Delta SASA_o$), by both shifting conformational equilibria toward open forms and lowering kinetic barriers of opening transitions. The results of this investigation demonstrate that small-amplitude motions linked to rapid O_2 migration are totally unaffected by predenaturational concentrations of Gdn or urea, whereas larger-amplitude structural fluctuations implicated in the slower penetration of bigger Qs are increasingly facilitated by the denaturant, to the point that in its presence the protein interior becomes also accessible to the largest solutes TA and SA. Quenching by these denaturant-induced large amplitude fluctuations tends to saturate within the experimental [Q] range, permitting the determination of the frequency of the underlying conformational transition.

For a quantitative examination of partial unfolding transitions, it is customary to express the dependence of kinetic and equilibrium constants on the denaturant concentration in terms of the respective m value, whose magnitude has been directly linked to the ΔSASA for the formation of the transition state or the open-gate conformer equilibrium, respectively.[49] Here, given the minimal number of points (2−3) available for the construction of the free energy plots and the uncertainty in the gate parameters, we can at best attempt a qualitative analysis of Gdn data. The Gdn m values relative to the linear quenching component (k_{ql}) and to the kinetic parameters k_o and k_c of the slow protein gate were estimated from the following free energy relationships

$$\ln[k_{ql}(D)/k_{ql}(0)] = \ln[K_o(D)/K_o(0)] = m[D]/RT \quad (12)$$

$$\ln[k_o(D)/k_o(0)] = m_o[D]/RT \quad (13)$$

$$\ln[\sigma(D)/\sigma(0)] = \ln[k_c(D)/k_c(0)] = m_c[D]/RT \quad (14)$$

In eq 12 we have adopted the molecular description (eq 9) for linear component k_{ql} ($k_{ql} = K_o k_{qo}$). In eqs 12 and 14, it is assumed that the open-gate quenching rate constant k_{qo} is not affected by the denaturant (i.e., $k_{qo}(D)/k_{qo}(0) = 1$). For the parameters K_o and k_c, we can only determine the change induced by Gdn, not their actual value. $m_s = m_o - m_c$ is the m value derived for the slow closed−open conformer equilibrium. R is the gas constant and T the absolute temperature. The m values estimates obtained from the data at 25 °C (Table 1) are reported in Table 3.

The linear component of the quenching reaction (k_{ql}) embodies segmental motions in the submillisecond and shorter time scale. The m value is negligibly small for O_2 indicating that structural fluctuations of this amplitude do not involve detectable variations in the protein surface area. For larger Qs the m value increases from 0.22 kcal mol^{-1} M^{-1} for AN (M_w = 53 Da) to 0.44 kcal mol^{-1} M^{-1} for acrylamide (M_w = 71 Da) and 0.30 kcal mol^{-1} M^{-1} for HA (M_w = 101 Da). It amounts to, respectively, about 4, 8, and 6% of the m value for global unfolding (m_U = 5.2 kcal mol^{-1} M^{-1}),[40] suggesting that the $\Delta SASA_o$ associated to these motions are in the range of 4−8% of the protein surface area exposed on complete unfolding of the macromolecule. Hence, beyond a given threshold amplitude, roughly the size of a diatomic molecule, protein motion requires some degree of

Table 3. m Values (kcal mol^{-1} M^{-1}) Relative to the Quenching Rate Constant of Azurin Phosphorescence in Gdn Solutions, at 25 °C, by Solutes Q of Increasing Molecular Size

Q	M_w	$m(k_o)$	$m(k_c)$	$m(K_o)$	$m(k_{ql})$
O_2	32	----	----	----	≈0
AN	53	----	----	----	0.225
acrylamide	71	0.32	−1.01	1.31	0.44
HA	101	0.77	−0.74	1.51	0.30
TA	175	0.88	−0.11	0.98	----
SA	206	1.06	−0.14	1.20	----
global unfolding [a]		3.68	−2.10	5.20	----

[a] From ref 40.

unfolding of the globular structure. Consistent with a more extensive disruption of bonding networks with higher amplitude structural fluctuations, $\Delta H^{\ddagger}(k_{ql})$ increases from about 10 kcal mol^{-1} for O_2 to 17−18 kcal mol^{-1} with acrylamide and HA.

The slow protein gate reveals conformational fluctuations in the 10−100 ms time scale and of sufficiently large amplitude to bring even the biggest quenchers within interaction range of W48. These motions decrease in frequency (k_o) with Q size (from 80 to 25 s^{-1}, from acrylamide to SA, in 1.3 M Gdn) and exhibit a progressively larger kinetic m value (m_o), from 0.32 kcal mol^{-1} M^{-1} of acrylamide to 1.06 kcal mol^{-1} M^{-1} of SA (Table 3). m_o is related to the change in SASA between the closed conformer and the transition state of the opening transition ($\Delta SASA_{TSo}$), and its magnitude ranges from 10 to 25% of the kinetic m value reported for global unfolding (3.68 kcal mol^{-1} M^{-1}). The value of m_c is negative, which is consistent with the fact that in the transition state less protein surface is exposed to the solvent than in the open conformer. Its magnitude is relatively large with acrylamide (−1.01 kcal mol^{-1} M^{-1}) and HA (−0.74 kcal mol^{-1} M^{-1}), over a third of that found for the global refolding rate (−2.1 kcal mol^{-1} M^{-1}),[40] but drops significantly with the largest quenchers TA (−0.11 kcal mol^{-1} M^{-1}) and SA (−0.14 kcal mol^{-1} M^{-1}). A difference in the kinetic m value patterns between intermediate size (acrylamide and HA) and large size (TA and SA) quenchers is probably indicative of distinct migration pathways for these groups of solutes, the structural fluctuation gating the access of the largest Qs being characterized by a more "open", largely hydrated transition state (the degree of solvent exposure in the transition state = $\Delta SASA_{TSo}/\Delta SASA_o = m_o/m_s$). Despite the differences in kinetics, the equilibrium m values ($m_s = m_o - m_c$) for the two groups of quenchers fall within a rather narrow range, between 1 and 1.5 kcal mol^{-1} M^{-1} (Table 3). Apparently, the $\Delta SASA_o$ of the corresponding open conformer, which is a sizable fraction, 20−30%, of that for whole molecule unfolding, is poorly correlated to the frequency (k_o) or the amplitude (up to 3-fold difference in Q size) of these motions, a finding that, if it were further confirmed, would caution on the danger of inferring dynamic information from equilibrium data, be it ΔG_o or m value, as is customary with HX studies in the EX2 regime.

CONCLUSIONS

The present exploratory study demonstrates a distinct and progressively greater influence of denaturants on native-state structural fluctuations in azurin that underlie the internal diffusion of solutes in the M_w range 51−206 Da. The relatively large m_s values reported here for protein-gated Q migration are at odds with the generally weak influence denaturants exerted on HX and SX exchange rates (k_{obs}) of buried NH and Cys targets,[31,32,36] even when disulfide reagents are twice the size of the largest Q employed here,[31] raising some concern that observed exchange rates (k_{obs}), rather than simply reflect the open-conformer equilibrium (K_o), are significantly affected by the local chemical reactivity of target and probe. This work illustrates potentialities and limitations of phosphorescence quenching for probing conformational dynamics, as well as its complementarity to HX and SX techniques. Among the limitations is the accessible time scale of protein motions, which is restricted to the subsecond lifetime of phosphorescence. Another is the inability to estimate conformer eqiulibria ($K_o = k_q/k_{qo}$) and associated free energy changes with sufficient accuracy. The reason is that the "open" conformer quenching rate constant, k_{qo}, is a sharp function of the distance of closest approach and is generally not known unless the target Trp becomes exposed to the solvent ($k_{qo} \approx 10^9$ M^{-1} s^{-1}). A further disadvantage of this approach relative to HX is that opposite mutants would need to be created in order to place the target Trp side chain in the desired site. On the positive side, it is possible to vary Q size and probe the amplitude spectrum of protein motions over a wide array. Also, for any Q a broad range of quenching rates is accessible simply by varying its concentration, a feature that occasionally permits to cross over from EX2 to EX1 reaction regimes and obtain directly the frequency of the rate-limiting structural fluctuation. Finally, the quenching interaction is not affected by chemistry. Unlike chemical exchange reactions that are sensitive to the local reactivity of target and probe, Q migration responds selectively to native-fold dynamics, a mandatory provision for unveiling subtle changes in protein dynamics as may occur upon varying experimental conditions (pH, ionic strength, stabilizing−destabilizing additives, etc.) that normally also affect chemical reactivity. Even at high denaturant concentrations, where a good fraction of the protein is unfolded and exchange reactions tend to be masked by the global unfolding transition, phosphorescence quenching reports specifically on local and subglobal structural fluctuations of the native state.

AUTHOR INFORMATION

Corresponding Author

*Tel.: +39 050 315 3046. Fax: +39 050 315 2760. E-mail: strambini@pi.ibf.cnr.it.

REFERENCES

(1) Shastry, M. C.; Roder, H. *Nat. Struct. Biol.* **1998**, *5*, 385.
(2) Travaglini-Allocatelli, C.; Cutruzzola, F.; Bigotti, M. G.; Staniforth, R. A.; Brunori, M. *J. Mol. Biol.* **1999**, *289*, 1459.
(3) Frederick, K. K.; Marlow, M. S.; Valentine, K. G.; Wand, A. J. *Nature* **2007**, *448*, 325.
(4) Wand, A. J. *Nat. Struct. Biol.* **2001**, *8*, 926.
(5) Eppler, R. K.; Hudson, E. P.; Chase, S. D.; Dordick, J. S.; Reimer, J. A.; Clark, D. S. *Proc. Natl. Acad. Sci. U.S.A.* **2008**, *105*, 15672.
(6) Hammes-Schiffer, S.; Benkovic, S. J. *Annu. Rev. Biochem.* **2006**, *75*, 519.
(7) Henzler-Wildman, K.; Kern, D. *Nature* **2007**, *450*, 964.
(8) Kale, S.; Ulas, G.; Song, J.; Brudvig, G. W.; Furey, W.; Jordan, F. *Proc. Natl. Acad. Sci. U.S.A.* **2008**, *105*, 1158.
(9) Loria, J. P.; Berlow, R. B.; Watt, E. D. *Acc. Chem. Res.* **2008**, *41*, 214.
(10) Wang, Y.; Berlow, R. B.; Loria, J. P. *Biochemistry* **2009**, *48*, 4548.
(11) Boehr, D. D.; Dyson, H. J.; Wright, P. E. *Biochemistry* **2008**, *47*, 9227.

(12) Bouvignies, G.; Bernado, P.; Meier, S.; Cho, K.; Grzesiek, S.; Bruschweiler, R.; Blackledge, M. *Proc. Natl. Acad. Sci. U.S.A.* **2005**, *102*, 13885.
(13) Bustamante, C. *Annu. Rev. Biochem.* **2008**, *77*, 45.
(14) Mittermaier, A.; Kay, L. E. *Science* **2006**, *312*, 224.
(15) Persson, E.; Halle, B. *J. Am. Chem. Soc.* **2008**, *130*, 1774.
(16) Lakowicz, J. R.; Weber, G. *Biochemistry* **1973**, *12*, 4171.
(17) Saviotti, M. L.; Galley, W. C. *Proc. Natl. Acad. Sci. U.S.A.* **1974**, *71*, 4154.
(18) Calhoun, D. B.; Englander, S. W.; Wright, W. W.; Vanderkooi, J. M. *Biochemistry* **1988**, *27*, 8466.
(19) Calhoun, D. B.; Vanderkooi, J. M.; Woodrow, G. V., 3rd; Englander, S. W. *Biochemistry* **1983**, *22*, 1526.
(20) Cioni, P.; Strambini, G. B. *J. Am. Chem. Soc.* **1998**, *120*, 11749.
(21) Cioni, P.; Strambini, G. B. *J. Mol. Biol.* **1999**, *291*, 955.
(22) Strambini, G. B. *Biophys. J.* **1987**, *52*, 23.
(23) Strambini, G. B.; Gonnelli, M. *Biochemistry* **2009**, *48*, 7482.
(24) Vanderkooi, J. M. Topics in Fluorescence Spectroscopy. In *Biochemical Applications*; Lakowicz, J. R., Ed.; Plenum: New Yok, 1991; Vol. 3, p 113.
(25) Strambini, G. B.; Gonnelli, M. *Biochemistry* **2011**, *50*, 970.
(26) Woodward, C. K.; Hilton, B. D. *Annu. Rev. Biophys. Bioeng.* **1979**, *8*, 99.
(27) Englander, S. W.; Kallenbach, N. R. *Q. Rev. Biophys.* **1984**, *16*, 521.
(28) Bai, Y.; Sosnick, T. R.; Mayne, L.; Englander, S. W. *Science* **1995**, *269*, 192.
(29) Arrington, C. B.; Robertson, A. D. *Biochemistry* **1997**, *36*, 8686.
(30) Clarke, J.; Itzhaki, L. S. *Curr. Opin. Struct. Biol.* **1998**, *8*, 112.
(31) Feng, Z.; Butler, M. C.; Alam, S. L.; Loh, S. N. *J. Mol. Biol.* **2001**, *314*, 153.
(32) Stratton, M. M.; Cutler, T. A.; Ha, J. H.; Loh, S. N. *Protein Sci.* **2010**, *19*, 1587.
(33) Bai, Y.; Milne, J. S.; Mayne, L.; Englander, S. W. *Proteins* **1993**, *17*, 75.
(34) Hvidt, A. *C. R. Trav. Lab. Carlsberg* **1964**, *34*, 299.
(35) Hvidt, A.; Nielsen, S. O. *Adv. Protein Chem.* **1966**, *21*, 287.
(36) Maity, H.; Lim, W. K.; Rumbley, J. N.; Englander, S. W. *Protein Sci.* **2003**, *12*, 153.
(37) Anderson, J. S.; Hernandez, G.; Lemaster, D. M. *Biochemistry* **2008**, *47*, 6178.
(38) Anderson, J. S.; Hernandez, G.; LeMaster, D. M. *Biophys. Chem.* **2009**, *141*, 124.
(39) Nar, H.; Messerschmidt, A.; Huber, R.; van de Kamp, M.; Canters, G. W. *FEBS Lett.* **1992**, *306*, 119.
(40) Sandberg, A.; Leckner, J.; Karlsson, B. G. *Protein Sci.* **2004**, *13*, 2628.
(41) Karlsson, B. G.; Pascher, T.; Nordling, M.; Arvidsson, R. H.; Lundberg, L. G. *FEBS Lett.* **1989**, *246*, 211.
(42) Strambini, G. B.; Kerwin, B. A.; Mason, B. D.; Gonnelli, M. *Photochem. Photobiol.* **2004**, *80*, 462.
(43) Strambini, G. B.; Gonnelli, M. *Biophys. J.* **2010**, *99*, 944.
(44) Strambini, G. B.; Cioni, P. *J. Am. Chem. Soc.* **1999**, *121*, 8337.
(45) Owen, C. S.; Vanderkooi, J. M. *Comments Mol. Cell. Biophys.* **1991**, *7*, 235.
(46) Strambini, G. B.; Gonnelli, M. *J. Phys. Chem. B* **2010**, *114*, 9691.
(47) Vanderkooi, J. M.; Englander, S. W.; Papp, S.; Wright, W. W.; Owen, C. S. *Proc. Natl. Acad. Sci. U.S.A.* **1990**, *87*, 5099.
(48) Wright, W. W.; Owen, C. S.; Vanderkooi, J. M. *Biochemistry* **1992**, *31*, 6538.
(49) Myers, J. K.; Pace, C. N.; Scholtz, J. M. *Protein Sci.* **1995**, *4*, 2138.